



HAL
open science

Chromatic Indices in the Normalized rgb Color Space

Martin Loesdau, Sébastien Chabrier, Alban Gabillon

► **To cite this version:**

Martin Loesdau, Sébastien Chabrier, Alban Gabillon. Chromatic Indices in the Normalized rgb Color Space. 2017 International Conference on Digital Image Computing: Techniques and Applications (DICTA), Nov 2017, Sydney, Australia. pp.1-8, 10.1109/DICTA.2017.8227415 . hal-03132308

HAL Id: hal-03132308

<https://upf.hal.science/hal-03132308>

Submitted on 5 Feb 2021

HAL is a multi-disciplinary open access archive for the deposit and dissemination of scientific research documents, whether they are published or not. The documents may come from teaching and research institutions in France or abroad, or from public or private research centers.

L'archive ouverte pluridisciplinaire **HAL**, est destinée au dépôt et à la diffusion de documents scientifiques de niveau recherche, publiés ou non, émanant des établissements d'enseignement et de recherche français ou étrangers, des laboratoires publics ou privés.

Chromatic Indices in the Normalized *rgb* Color Space

Martin Loesdau, Sébastien Chabrier, Alban Gabillon

Laboratoire Géopôle du Pacifique Sud EA4238
Université de la Polynésie française
Punaauia, Tahiti

Abstract—*In typical applications, chromatic indices are calculated as linear combinations of the normalized r -, g - and b -channels and used as features for a later classification based on chromatic appearance. But the variety of indices used in the literature is very limited. Furthermore is the choice of which index to use justified either empirically, based on false mathematical assumptions or not justified at all. The reason for the lack of mathematical justification is that so far no formal definition of chromatic indices existed. Such a definition is provided in this paper. An experimental classification with 180 different index combinations shows that the index choice has a significant impact on the classification. The results stand in sharp contrast to the very limited variety of indices used in the literature. The results imply the need for deterministic methods to estimate ideal indices for a given application, for which we hope the provided formalization might be useful.*

Keywords—*color space theory, normalized rgb color space, chromatic indices, color object classification, color feature vectors*

I. INTRODUCTION

While the RGB color model is based on the human biological processing of color in the retina, the HS color model is based on the human color perception [1]. The normalized *rgb* color space combines both properties by separating achromatic from chromatic information (perceptual model), while preserving the proportional relations of the entries of the original RGB data (biological model). In computer vision, the normalization of RGB vectors is often used as an intermediate step, followed by the creation of chromatic indices described as linear combinations of the normalized color channels r , g and b . Applications comprise for example vehicle color recognition [2], food inspection [3], [4], skin detection [5]-[7], color texture analysis [8] or object tracking [9].

More generally, chromatic indices are often used as features for object, image or image region classification. But the theoretically unlimited possibilities of chromatic index generation are only poorly exploited. By far the most used indices are the pure r - and g -channel, as for example for skin detection in [5]-[7] and [10]-[12]. The very same two indices are used in [2] for vehicle color recognition, in [3] for the classification of pizza toppings, in [13] for building recognition, in [8] and [14] for color-texture analysis (artificial

image as well as real scenes comprising outdoor and indoor), in [9] for object tracking (civil and military vehicles), in [15] for image segmentation (artificial images and real scenes) or in [16] for image region recognition (real scenes). Even though in many of the cited papers, features of other color models or other feature types such as shape or greylevel gradients are added, the use of the same chromatic indices for objects, images or image regions with a completely different data distribution contradicts sharply the general consensus in the domain of classification that “A key ingredient in the design of visual object classification systems is the identification of relevant class specific aspects [...]” [17]. It is highly unlikely that the same two chromatic indices r and g correlate ideally with every single one of all the mentioned objects, images or image regions in means of their chromatic appearance. This hypothesis is bolstered by publications in which indeed application specific indices are used, such as for example the ‘excessive green index’ ($2g-r-b$) [18] or the ‘excessive red index’ ($1.4r-g$, or rather excessive green – excessive red = $g-2.4r-b$) [19] for plant recognition or the ‘opposed’ index $r-b$ for outdoor scene recognition under consideration of season and illumination change [20]. The main question is accordingly, which is the ideal index or which are the ideal indices for a given application? So far, the indices used in the literature are mostly applied based on empirical/experimental justifications [7], [12], [18]-[20], false mathematical assumptions [3], [5], [16], [21] (will be explained in section IV) or with no justification at all [2], [8], [9], [14]. This does not necessarily mean that the used indices are not ideal, nor is it meant as a critic; the problem is that, so far, there is no mathematical method to determine an ideal chromatic index for a given application. One reason for the lack of mathematical justification is certainly that no formal method for a consistent chromatic index generation exists. After briefly introducing the concept of RGB vector normalization in section II, such a formalization of chromatic index generation will be developed in section III. It will be shown that any possible chromatic index described by a linear combination of the chromatic channels r , g and b can be described by a single parameter α that corresponds to the perceptual chromatic parameter Hue. The formalization implies that infinite chromatic indices can be generated. To evaluate if and to which degree different indices impact on color object classification, an experimental classification with 180 different index constellations was

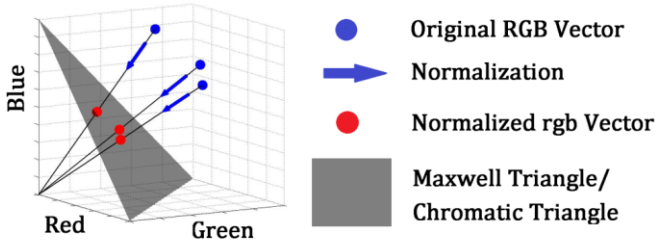


Figure 1: Normalizing RGB vectors to reduce illumination information by projecting them to the Maxwell triangle.

applied to the ETH80 cropped close image database [22]. After briefly introducing histogram binning of chromatic indices in section IV (along with a clarification of a common misinterpretation of chromatic channel redundancy), the experiment methodology is explained in section V. Results are presented and discussed in section VI, followed by the conclusion in section VII

II. THE NORMALIZED *RGB* COLOR SPACE

In the definition of the HS color spaces as proposed by Joblove and Greenberg [23], Hue and Saturation of an RGB vector do not change when shifted along a line through origin and the normal vector itself. A separation of achromatic and chromatic components in this definition can hence be reached by normalizing an RGB vector with the sum of its entries as to

$$\begin{bmatrix} r \\ g \\ b \end{bmatrix} = \begin{bmatrix} R \\ G \\ B \end{bmatrix} / (R + G + B). \quad (1)$$

The normalization results in a shift of an RGB vector along a line through origin and the vector itself to a plane with normal $[1 \ 1 \ 1]$ going through point $[1/3 \ 1/3 \ 1/3]$ (Figure 1). The plane is cut by the borders of the RGB cube into an equilateral triangle, often referred to as chromatic triangle or Maxwell triangle [24]. The normalized *rgb* vectors contain all chromatic information in the definition of the HS spaces, while the proportional relation of its entries, one of the basic concepts of the RGB color model, is preserved.

The projection of RGB vectors on a single plane results in a dimensionality reduction which is in the literature typically exploited by projecting the Maxwell triangle to the RG-plane [24]. In this paper, the Maxwell triangle is rotated as shown in

Figure 2; the coordinates of the rotated *rgb* vectors can be obtained by conversion from Barycentric to Euclidian coordinates as to

$$\begin{bmatrix} x \\ y \end{bmatrix} = \sqrt{2} \begin{bmatrix} \frac{g-r}{\sqrt{3}} \\ \frac{2}{3} - r - g \end{bmatrix}. \quad (2)$$

All following subjects can be derived either from the RGB space, the projected Maxwell triangle or the rotated one. In this paper, the formalization of chromatic indices of the next section will be done within the RGB geometry to illustrate the geometrical relation between RGB and normalized *rgb* space. As in the authors' opinion the relation between RGB space and rotated Maxwell triangle are more intuitive than between RGB space and projected Maxwell triangle (mostly because of the preservation of the threefold rotational symmetry around the achromatic axis in regards of the space topology), the former will be used for illustration of mathematical properties within the figures of the remaining sections.

III. FORMALIZATION OF CHROMATIC INDICES IN THE NORMALIZED *RGB* COLOR SPACE

All chromatic indices described as linear combinations of normalized *rgb* color channels can be seen as dot product of a normalized *rgb* vector and a 3-dimensional vector:

$$r = \begin{bmatrix} 1 \\ 0 \\ 0 \end{bmatrix} \cdot \begin{bmatrix} r \\ g \\ b \end{bmatrix}; \quad 1.4r - g = \begin{bmatrix} 1.4 \\ -1 \\ 0 \end{bmatrix} \cdot \begin{bmatrix} r \\ g \\ b \end{bmatrix}. \quad (3)$$

Hence, each index can be seen as a scaled distance measurement between a normalized *rgb* vector and a plane with a normal described by the chromatic index going through point $[0 \ 0 \ 0]$ (scaled as the indices found in the literature are usually not normalized by its l_2 -norm). As the normalized *rgb* vectors lie all on a plane (the Maxwell triangle), an equivalent distance measurement to a given index can be done with a transformed index described by a vector whose element sum is zero:

For an arbitrary chromatic index described by a vector p , the

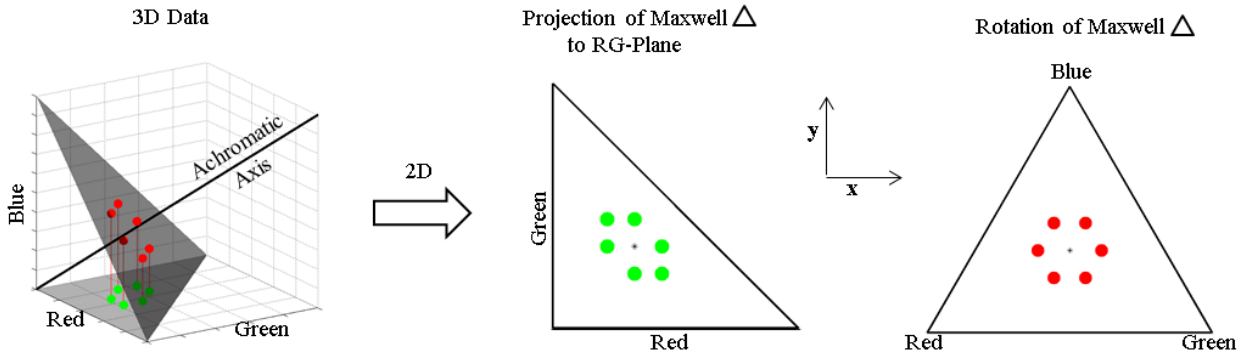


Figure 2: Normalized *rgb* vectors (all 6 permutations of $[10 \ 15 \ 20]$ projected to the Maxwell triangle) in the RGB space (left), their "classical" 2D representation in the RG-plane (middle) and in the rotated Maxwell triangle (right).

scaled distance d , as described above, can be written as dot product between vector p and the normalized rgb vector:

$$d = \begin{bmatrix} p_1 \\ p_2 \\ p_3 \end{bmatrix} \cdot \begin{bmatrix} r \\ g \\ b \end{bmatrix}. \quad (4)$$

Transforming vector p so that the sum of its entries equals zero means shifting it to a plane through origin with normal $[1 \ 1 \ 1]$. The so obtained scaled distance d_2 is

$$d_2 = \left(\begin{bmatrix} p_1 \\ p_2 \\ p_3 \end{bmatrix} - \begin{bmatrix} 1 \\ 1 \\ 1 \end{bmatrix} \frac{(p_1 + p_2 + p_3)}{3} \right) \cdot \begin{bmatrix} r \\ g \\ b \end{bmatrix} \quad (5)$$

which can be written as

$$d_2 = \left(\begin{bmatrix} p_1 \\ p_2 \\ p_3 \end{bmatrix} \right) \cdot \begin{bmatrix} r \\ g \\ b \end{bmatrix} - \begin{bmatrix} 1 \\ 1 \\ 1 \end{bmatrix} \frac{(p_1 + p_2 + p_3)}{3} (r + g + b) \quad (6)$$

As the sum of entries of a normalized rgb vector is 1, the relation between distance d obtained by the original index and distance d_2 obtained by shifting the original index to a plane through origin with normal $[1 \ 1 \ 1]$ is

$$d_2 + \frac{(p_1 + p_2 + p_3)}{3} = d \quad (7)$$

This means that shifting vector p to a plane through origin with normal $[1 \ 1 \ 1]$ results in a linear shift of the distance obtained with the original chromatic index. Hence, without loss of information, an index that is described by a linear combination of rgb channels can as well be described with a vector n whose sum of elements equals 0:

$$d_n = n_1 r + n_2 g + n_3 b \quad (8)$$

with $n_1 + n_2 + n_3 = 0$.

As the sum of elements of vector n is zero, all n are perpendicular to the achromatic axis. If the condition that vector n is normalized with the l_2 -norm is added (a scaling that does not change the information content), each vector n can be expressed by a vector n_0 rotated around the achromatic axis by a certain angle α .

$$\vec{n}_\alpha = \bar{R}_{\alpha, [1 \ 1 \ 1]} \vec{n}_0. \quad (9)$$

In this equation R is the 3-dimensional rotation matrix. If the initial vector n_0 is pointing in the direction of the red-axis, and the rotation is counterclockwise in respect to the rotated Maxwell triangle, any vector n_α complying with Eq.8 can be expressed as

$$\vec{n}_\alpha = \sqrt{\frac{2}{3}} \begin{bmatrix} \cos \alpha \\ \cos(\alpha - 120^\circ) \\ \cos(\alpha + 120^\circ) \end{bmatrix} \quad (10)$$

which can be obtained by expanding Eq. 9 and simplifying the

trigonometric terms.

By inserting Eq10 in Eq. 8, any chromatic index that is described as a linear combination of rgb channels can now be expressed as

$$d_\alpha = \sqrt{\frac{2}{3}} (\cos(\alpha) r + \cos(\alpha - 120^\circ) g + \cos(\alpha + 120^\circ) b). \quad (11)$$

With Eq. 11 any chromatic index that is described as a linear combination of normalized rgb channels can be calculated based on a single parameter α . As this parameter describes a rotation around the achromatic axis it corresponds to the human perceptual parameter Hue in the definition of the HS spaces [23].

As the sum of a normalized rgb vector is 1, Eq. 11 can be simplified to

$$d_\alpha = \sqrt{\frac{2}{3}} \cos(\alpha) + \sqrt{2} (g \sin(\alpha - 60^\circ) - b \sin(\alpha + 60^\circ)) \quad (12)$$

and by substituting

$$d_{H,\alpha} = \frac{d_\alpha}{\sqrt{2}} + \frac{1}{\sqrt{3}} \cos(\alpha), \quad (13)$$

a scaling and a shift that does not change the information content of the index further to

$$d_{H,\alpha} = g \sin(\alpha - 60^\circ) - b \sin(\alpha + 60^\circ). \quad (14)$$

Typically, chromatic indices are normalized to a range of $[0, 1]$, which can be done by normalizing with minimum and maximum of the index in regards of a chosen α as to

$$d_{H,\alpha} = \frac{d_{H,\alpha} - \min_{d_{H,\alpha}}}{\max_{d_{H,\alpha}} - \min_{d_{H,\alpha}}}, \quad d_{H,\alpha} \in [0,1] \quad (15)$$

with minimum $\min_{d_{H,\alpha}}$ and maximum $\max_{d_{H,\alpha}}$ at two of the three vertices of the Maxwell triangle:

$$\min_{d_{H,\alpha}} = \min(0, \sin(\alpha - 60^\circ), -\sin(\alpha + 60^\circ)) \quad (16)$$

$$\max_{d_{H,\alpha}} = \max(0, \sin(\alpha - 60^\circ), -\sin(\alpha + 60^\circ)). \quad (17)$$

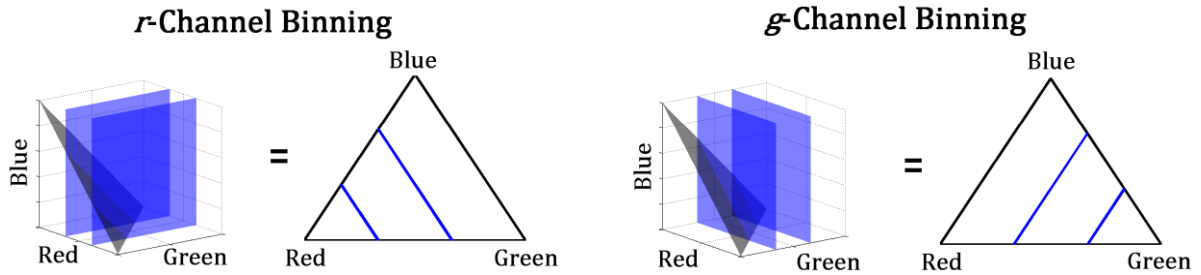


Figure 3: r -channel binning in 3 bins in the RGB space and in the rotated Maxwell triangle (left) and the equivalent g -channel binning (right).

Eqs. 15-17 give a consistent and compact description of any possible chromatic index in the normalized rgb space, meaning any linear combination of r -, g -, and b -channel.

As a last remark before concluding this section, it is noted that

$$d_{H,\alpha} = 1 - d_{H,\alpha+180^\circ} \quad (18)$$

which means that it is sufficient to choose α in a range of $[0^\circ, 179^\circ]$ which covers every possible chromatic index in the normalized rgb color space.

IV. CHROMATIC INDICES USED WITH HISTOGRAMS FOR COLOR OBJECT CLASSIFICATION

A very typical application of chromatic indices is their use in combination with histograms [2]-[9]. The additional step of histogram binning is added to obtain a normalized and comparable quantization of the chromatic properties of an object, image or image region [26], [27]. In the following, histograms in its basic form with equidistant non-overlapping bins are considered. Here, the data space is divided in equidistant regions and the data occurrence frequency in every

region is counted. Afterwards the frequency is divided by the total amount of data so that data sets of different sizes can be compared.

A visualization of the geometrical properties of binning chromatic indices in the original RGB space and in the rotated Maxwell triangle can be seen in Figure 3. As a chromatic index is a distance measurement to a plane in the original RGB space, histogram binning corresponds to a separation of the RGB space with (equidistant) planes parallel to the one that is defined by the chromatic index itself. Equivalently, as the planes intersect with the Maxwell triangle in lines, binning chromatic indices in the rotated Maxwell triangle corresponds to a separation of the triangle by parallel lines.

A common misinterpretation of the geometrical properties of chromatic indices in the normalized rgb color space in combination with histogram binning is that channel redundancy implies histogram redundancy. In [3], [5], [16], [21] it is argued that the sum of the entries of a normalized rgb vector is 1. This redundancy (one channel can be expressed by the remaining two) is used to justify the choice of rg -binning instead of for example gb -binning or even rgb -binning. But the used histograms are 2-dimensional, which means the

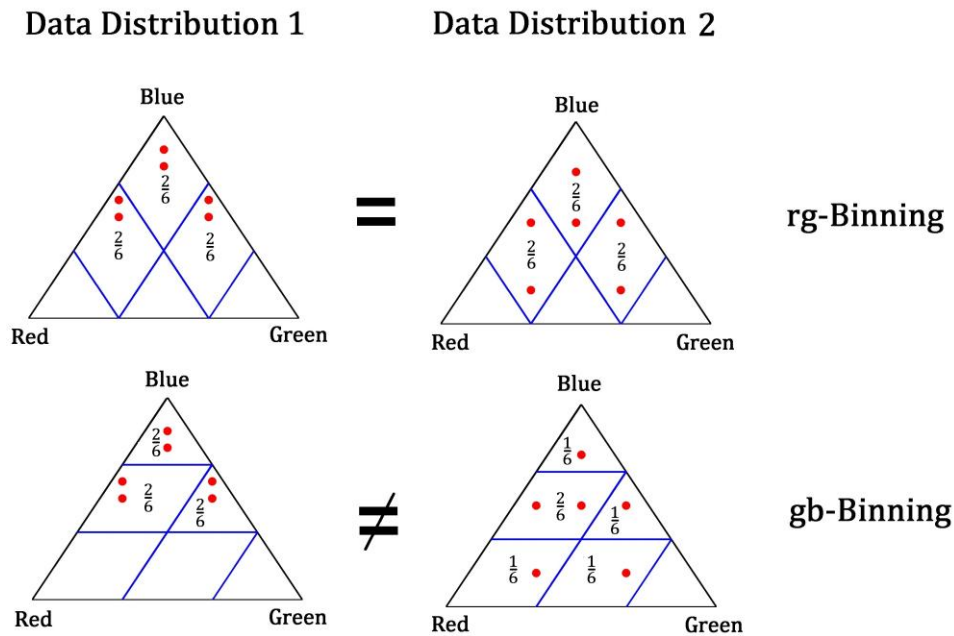


Figure 4: Schema of two different data distributions (first column and second column) resulting in the same histogram distribution when rg -binning is applied with three equidistant bins per channel (first row) but different histogram distribution when gb -binning is applied (second row).

redundancy applies only in a way that if for example the rg -histogram and the gb -histogram are given, the rb -histogram can be derived from the distribution of the former two.

In Figure 4 rg -binning (top row) and gb -binning (bottom row) is done for two different hypothetical data sets (left and right column). The red dots represent data points (normalized rgb vectors). If for the data distribution of the left column a 2-dimensional rg -histogram with 3 bins per channel is calculated, 3 histogram entries are non-zero, each representing $\sim 33\%$ of the data (top left). The same rg -histogram is obtained for the 2nd data distribution (top right). For a gb -binning of the two data distributions instead (bottom row) two different histograms are obtained. This means that there is no bijective relation between rg and gb histograms. In other words, it does make a difference if rg -binning, or gb -binning, or rb -binning is applied.

But more importantly, the common implication that there is only the choice between those three possibilities does not at all correspond to the nature of chromatic indices. On the contrary, there are infinite possibilities and they should somehow be considered if the hypothesis that an ideal index or an ideal combination of indices for a given application exists, as developed in the introduction, holds. This hypothesis can as well be expressed as assumption that changing an index in a given classification has an impact on the classification result. To explore if this assumption is valid, we applied an experimental classification with a brute force evaluation of the impact of varying indices, as will be explained in the following section.

V. EXPERIMENTS

To evaluate if and to which extend different chromatic indices have an influence on color object classification, we applied classical histogram comparison to the ETH-80 cropped close image database. The database consists of 8 different classes (Figure 5), comprising 10 different objects each. Each object is represented by 41 images taken under the same illumination conditions but from different view angles. It is important to note that this experimental classification has the purpose of proving the hypothesis that changing an index in a given classification has an impact on the classification result rather than to provide an ideal classification of the given ETH-80 database (such a classification would need additional

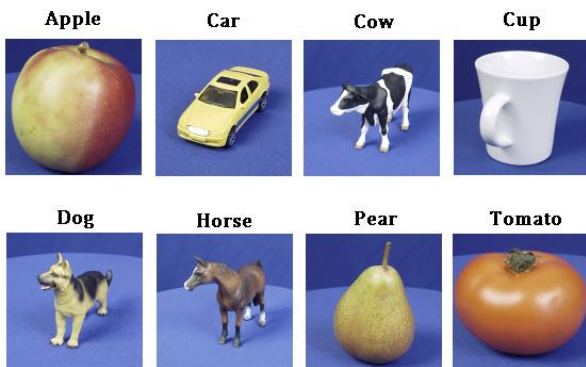


Figure 6: Example images of one object of each of the 8 ETH-80 database classes.

features such as for example local shape, global shape or texture [22]). Implementing the here presented color-theoretical aspects for color object classification based on human perception is part of our current work.

A. Histogram Configuration

For each segmented image of the ETH-80 database, 180 chromatic index calculations according to Eq. 15 were applied with a Hue α ranging from 0° to 179° with a 1° increment. Each index was binned in 64 equidistant bins over the whole possible range of the index ($[0, 1]$). Out of the obtained indices 180 histograms were calculated, each one a concatenation of the 1D histograms of two different indices. The difference between the α of two indices of each histogram was set to 120° . This configuration was chosen, as it comprises classical index combinations such as 0° and 120° that corresponds to rg -binning, 120° and 240° (resp. its equivalent 60°) that corresponds to gb -binning and 240° (resp. its equivalent 60°) and 0° that corresponds to rb -binning,

B. Classification

180 separate classifications, one for each concatenated histogram was done. The applied procedure corresponds to the methodology described in [25]. A leave-one-object-out cross validation was done by calculating the χ^2 distance between a given image of an object and all images of all remaining objects. The class of the given image was determined by the class of the image with the minimal distance to the given one.

VI. RESULTS AND DISCUSSION

Within the following subsections the classification results will be analyzed on three abstraction level: the global classification performance, the classification performance per class and the classification performance per object.

A. Global Performance

The global classification was calculated as percentage of all images correctly labeled per used histogram constellation. The results are shown in Figure 6. The angle α on the abscissa describes the Hue of the first of the two chromatic indices used per histogram configuration (the second is $\alpha+120^\circ$). Firstly, it can be seen that the classification results at 0° (rg -binning), 60° (rb -binning) and 120° (gb -binning) are not the same, again disproving the assumption that channel

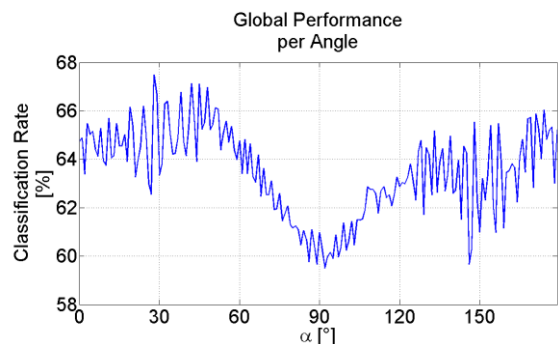


Figure 5: Global classification performance over all 180 different histogram constellations of the ETH-80 data base.

redundancy implicates histogram redundancy in the case of the use of one 2D histogram. Secondly, a general variation of the global classification depending on the used chromatic indices can be observed. This variation supports the hypothesis that the descriptive power of chromatic indices is application dependent. It can be observed further, that the maximum global classification is at 28° (second index 188°) which corresponds to chromatic indices that have so far not been applied in standard approaches.

B. Performance per Class

In Figure 8 (next page), the classification performance of each class of the ETH-80 database is shown over all 180 different histogram constellations. The performance was calculated as percentage of correctly labeled images of one class. Here as well, a variation of the classification can be observed for each one of the classes with a difference between minimum and maximum classification rate of up to 30% (class ‘car’). Furthermore are the optima of different classes at different histogram constellations, which indicates that the descriptive power of chromatic indices does depend on the class constitution.

C. Performance per Object

To evaluate the classification performance per object, the percentage of correctly classified images of all 41 images of each object for all 180 histogram constellations was calculated. In Figure 7, the maximum (blue) and minimum (green) classification rate of all 180 histogram classifications are shown per object. For almost every object a significant difference between minimum and maximum classification can be observed, with a difference of up to 100% (within class ‘horse’). The difference of 100% means that with a certain histogram constellation all 41 images of the corresponding object were correctly labeled, while with another one no image of this object was labelled correctly.

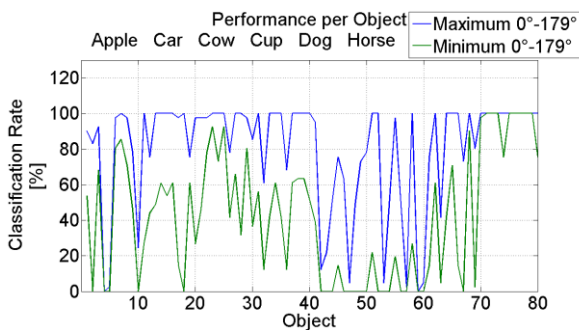


Figure 7: Minimum classification performance (green) and maximum performance (blue) of each of the 80 objects (10 objects per class) of the ETH-80 database.

D. Summary

The presented results show that on every level of classification, the choice of chromatic indices has a significant impact on the obtained classification rate. A variation of classification accuracy can be observed over the whole range

of used indices. The results indicate that the descriptive power of chromatic indices strongly depend on the data distribution they are applied to. These results stand in sharp contrast to the very limited variety of indices used in the literature. They stand especially in sharp contrast to the standard application of *rg*-histogram binning on different applications such as skin detection, car color classification, color texture classification, building recognition and so on, as mentioned in section I. Furthermore, it could be seen that the classification results of *rg*-binning, *gb*-binning and *rb*-binning are not identical, which stands in contrast to implications found in the literature (as explained in section IV).

Generally, the results show that the potential of normalized *rgb* chromatic indices is yet not at all fully exploited. In the shown experiments two indices were used per classification. But the amount of two was only chosen to correspond to the standard applications of chromatic indices in the literature. So was the choice of the difference of 120° between two indices. Theoretically, the ideal number of indices and their geometrical relation to each other depend on the data distribution and have hence to be determined according to a specific application. Therefore, suitable deterministic methods have to be evaluated or developed that consider the global data distribution of an application as well as inter- and intraclass correlation aspects.

VII. CONCLUSION

The normalized *rgb* color space is an interesting space as it combines the RGB color model that is based on the human biological processing of color with the HS model that is based on the human perception of color. Applications of this space can be found in almost any domain of color object, image or image region classification. A typical application is to calculate chromatic indices that are described by linear combinations of the three normalized color channels *r*, *g* and *b*. But so far the variety of indices has been very limited. Indices found in the literature are limited to the pure channels *r*, *g*, and *b*, the opposed indices *r-g*, *g-b*, *r-b* and some application specific feature such as ‘excessive green’ or ‘excessive red’. Furthermore is the choice of which index to use justified either empirically/ experimentally, based on false mathematical assumptions or not justified at all. The reason for the lack of mathematical justification is that so far no formal definition of chromatic indices existed. Such a definition was developed in this paper. It could be shown that every chromatic index that is described by a linear combination of the normalized color channels can be described by a single parameter α that corresponds to the human perceptual parameter Hue. The formalization implies that theoretically infinite indices can be generated. An experimental histogram-based classification for 180 different chromatic index combinations showed that the index choice has a significant impact on the global classification rate, as well as on the classification rate of each class, each object and each image. These results stand in sharp contrast to the limited variety of indices so far used in the literature. The results show the need for a deterministic estimation of application-specific

indices. The formalization of chromatic indices in this paper opens the possibility to evaluate or develop deterministic methods to find ideal indices or index combinations for a given application.

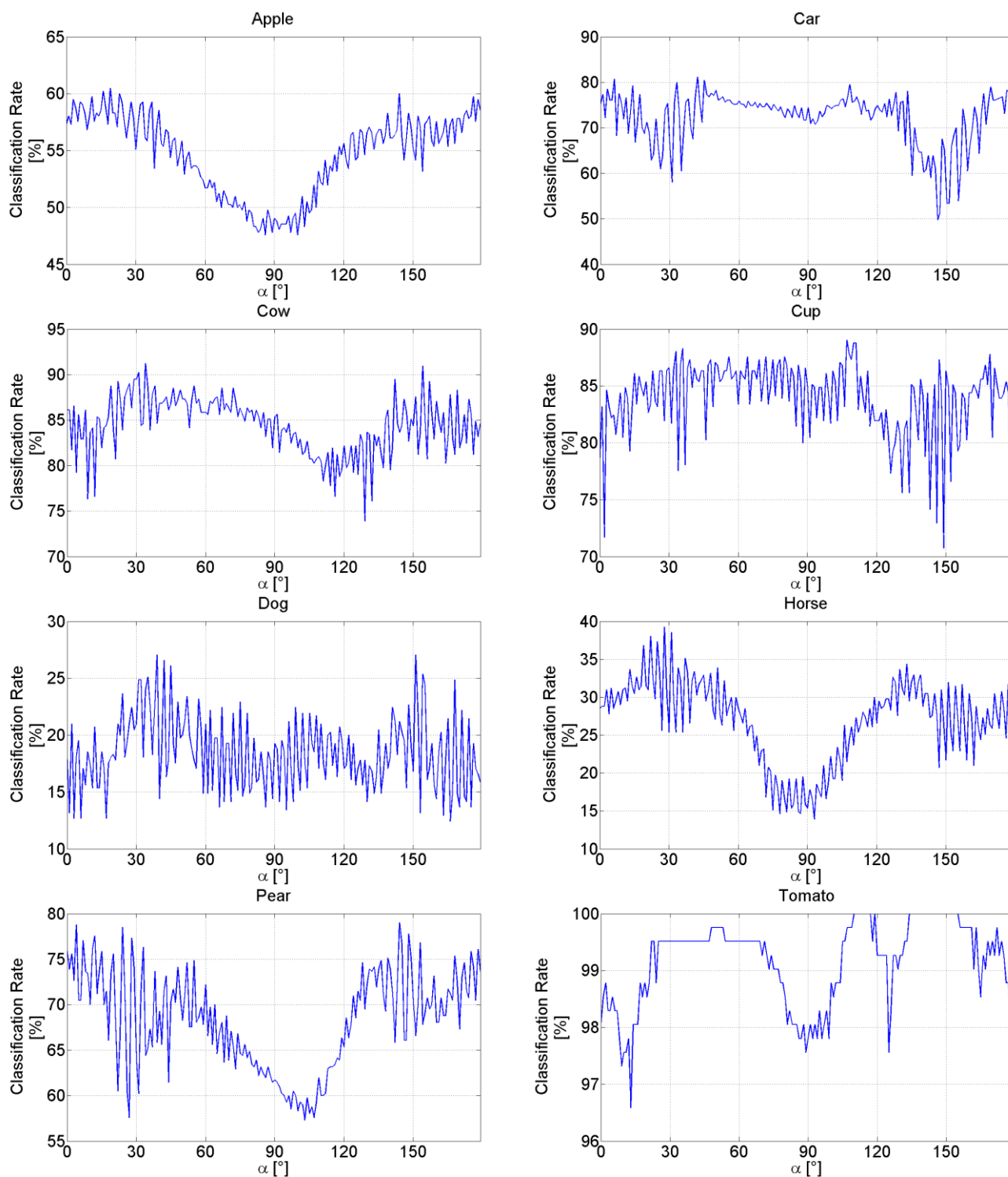


Figure 8: Classification performance of each of the 8 classes of the ETH-80 database over all 180 histogram constellations.

REFERENCES

- [1] Loesdau, M., Chabrier, S., Gabillon, A.: Hue and Saturation in the RGB Color Space. In proceedings of: 6th International Conference, ICISP, France, 2014. Lecture Notes in Computer Science, Volume 8509, pp 203-212.
- [2] Chen, P., Bai, X., & Liu, W.: Vehicle color recognition on urban road by feature context. *IEEE Transactions on Intelligent Transportation Systems*, 15(5), 2340-2346, 2014.
- [3] Du, C. J., & Sun, D. W.: Comparison of three methods for classification of pizza topping using different colour space transformations. *Journal of Food Engineering*, 68(3), 277-287, 2005.
- [4] Font, D., Tresanchez, M., Pallejà, T., Teixidó, M., Martínez, D., Moreno, J., & Palacín, J.: An image processing method for in-line nectarine variety verification based on the comparison of skin feature histogram vectors. *Computers and Electronics in Agriculture*, 102, 112-119, 2014.
- [5] Yang, J., & Waibel, A.: Tracking human faces in real-time (No. CMU-CS-95-210). Carnegie-Mellon Univ Pittsburgh Pa School Of Computer Science, 1995.
- [6] Lee, J. Y., & Yoo, S. I.: An elliptical boundary model for skin color detection. In *Proc. of the 2002 International Conference on Imaging Science, Systems, and Technology*, 2002.
- [7] Hassanat, A. B., Alkasassbeh, M., Al-awadi, M., & Esra'a, A.: Colour-based lips segmentation method using artificial neural networks. In *Information and Communication Systems (ICICS)*, 2015 6th International Conference on, IEEE, 188-193, 2015.
- [8] Mäenpää, T., & Pietikäinen, M.: Classification with color and texture: jointly or separately?. *Pattern recognition*, 37(8), 1629-1640, 2004.
- [9] Wang, J., & Yagi, Y.: Integrating color and shape-texture features for adaptive real-time object tracking. *IEEE Transactions on Image Processing*, 17(2), 235-240, 2008.
- [10] Vezhnevets, V., Sazonov, V., & Andreeva, A.: A survey on pixel-based skin color detection techniques. In *Proc. Graphicon (Vol. 3, pp. 85-92)*, 2003.
- [11] Kakumanu, P., Makrogiannis, S., & Bourbakis, N.: A survey of skin-color modeling and detection methods. *Pattern recognition*, 40(3), 1106-1122 2007.
- [12] Soriano, M., Martinkauppi, B., Huovinen, S., & Laaksonen, M.: Adaptive skin color modeling using the skin locus for selecting training pixels. *Pattern Recognition*, 36(3), 681-690, 2003.
- [13] Groeneweg, N. J., de Groot, B., Halma, A. H., Quiroga, B. R., Tromp, M., & Groen, F. C.: A fast offline building recognition application on a mobile telephone. In *International Conference on Advanced Concepts for Intelligent Vision Systems (pp. 1122-1132)*. Springer Berlin Heidelberg, 2006.
- [14] Cernadas, E., Fernández-Delgado, M., González-Rufino, E., & Carrión, P.: Influence of normalization and color space to color texture classification. *Pattern Recognition*, 61, 120-138, 2017.
- [15] Busin, L., Vandenbroucke, N., & Macaire, L.: Color spaces and image segmentation. *Advances in imaging and electron physics*, 151(1), 1, 2008.
- [16] Zhu, C., Bichot, C. E., & Chen, L.: Image region description using orthogonal combination of local binary patterns enhanced with color information. *Pattern Recognition*, 46(7), 1949-1963, 2013.
- [17] Gehler, P., Nowozin, S.: "On feature combination for multiclass object classification." 2009 IEEE 12th International Conference on Computer Vision. IEEE, 2009.
- [18] Woebbecke, D. M., Meyer, G. E., Von Bargen, K., Mortensen, D. A.: Color indices for weed identification under various soil, residue, and lighting conditions. *Transactions of the ASAE-American Society of Agricultural Engineers*, 38(1), 259-270, 1995.
- [19] Meyer, G. E., & Neto, J. C.: Verification of color vegetation indices for automated crop imaging applications. *Computers and Electronics in Agriculture*, 63(2), 282-293 2008.
- [20] Mori, H., Kobayashi, K., Ohtuki, N., & Kotani, S.: Color impression factor: an image understanding method for outdoor mobile robots. In *Intelligent Robots and Systems, 1997. IROS'97., Proceedings of the 1997 IEEE/RSJ*
- [21] Van De Sande, K., Gevers, T., & Snoek, C.: Evaluating color descriptors for object and scene recognition. *IEEE transactions on pattern analysis and machine intelligence*, 32(9), 1582-1596, 2010.
- [22] Leibe, B., & Schiele, B.: Analyzing appearance and contour based methods for object categorization. In *Computer Vision and Pattern Recognition, 2003. Proceedings. 2003 IEEE Computer Society Conference on (Vol. 2, pp. II-409)*. IEEE, 2003.
- [23] Joblove, G. H., & Greenberg, D.: Color spaces for computer graphics. In *ACM siggraph computer graphics (Vol. 12, No. 3, pp. 20-25)*. ACM, 1978.
- [24] Wyszecki, G., & Stiles, W. S.: *Color science (2nd edition)*. New York: Wiley, 2000.
- [25] Leibe, B., & Schiele, B.: Analyzing appearance and contour based methods for object categorization. In *Computer Vision and Pattern Recognition, 2003. Proceedings. 2003 IEEE Computer Society Conference on (Vol. 2, pp. II-409)*. IEEE, 2003.
- [26] Thaper, N., Guha, S., Indyk, P., & Koudas, N.: Dynamic multidimensional histograms. In *Proceedings of the 2002 ACM SIGMOD international conference on Management of data (pp. 428-439)*. ACM, 2002.
- [27] Swain, M. J., & Ballard, D. H.: Color indexing. *International journal of computer vision*, 7(1), 11-32, 1991.